physica status solidi

pss

www.interscience.wiley.com

reprints

www.pss-rapid.com

www.pss-c.com

www.pss-b.com

www.pss-a.com

WILEY-VCH

REPRINT

Phys. Status Solidi B **246**, No. 11–12, 2581–2585 (2009) / **DOI** 10.1002/pssb.200982266

physica status solidi b
www.pss-b.com
basic solid state physics

Exciton energy calculations for single wall carbon nanotubes

R. Saito*[,1], K. Sato[2], P. T. Araujo[3], A. Jorio[3], G. Dresselhaus[4], and M. S. Dresselhaus[5]

[1] Department of Physics, Tohoku University, Sendai 980-8578, Japan
[2] Department of Mechanical Engineering, School of Engineering, The University of Tokyo, Tokyo 113-8656, Japan
[3] Departamento de Física, Universidade Federal de Minas Gerais, Belo Horizonte, MG 30123-970, Brazil
[4] Department of Electrical Engineering and Computer Science, Department of Physics, Massachusetts Institute of Technology, Cambridge, MA 02139-4307, USA
[5] Francis Bitter Magnet Laboratory, Massachusetts Institute of Technology, Cambridge, MA 02139-4307, USA

Received 28 April 2009, revised 29 June 2009, accepted 14 August 2009
Published online 12 October 2009

PACS 71.35.Cc, 78.30.Na, 78.67.Ch

* Corresponding author: e-mail rsaito@flex.phys.tohoku.ac.jp, Fax: +81-22-795-6447

Using the Bethe–Salpeter equation, we have calculated the exciton energies of (i) bright exciton states; (ii) 2g exciton energies; and (iii) the energy difference between dark and bright exciton states for single wall carbon nanotubes (SWNTs) as a function of diameter. By adjusting the dielectric constant, we can reproduce the observed exciton energies in the resonance Raman spectra and two-photon absorption spectra for SWNTs. The environmental effect on the transition energies can be explained by a diameter-dependent dielectric constant. However, the energy difference between the dark and bright exciton states cannot be reproduced simply by changing the dielectric constant consistently. Thus we need to consider the evaluation of the Coulomb interaction, especially with regard to the surrounding materials.

1 Introduction In photoluminescence (PL) and resonance Raman spectra (RRS), the optical transition energies of a single wall carbon nanotube (SWNT) have unique values depending on the SWNT geometrical structure, which is useful for characterizing the chirality of SWNTs, specified by its two integers (n, m) [1]. When the polarization of the incident light is parallel to the nanotube axis, the optical selection rule allows the dipole transition from the i-th valence energy band to the i-th conduction energy band, E_{ii}, where i is the subband index measured from the Fermi energy. The E_{ii} energy values are generally plotted as a function of the diameter d_t of (n, m) SWNTs, which is called the Kataura plot [2, 3]. The Kataura plot has been frequently used in RRS. In the Kataura plot we can assign (n, m) values for given information of the laser excitation energy E_L and the diameter information which is obtained by the radial breathing mode (RBM) frequency. However, E_{ii} values shift with both red and blue shifts up to 100 meV, depending on the surrounding materials or on the type of semiconductor (type I or II) SWNT, and these shifts are known as the environmental effect [4–7]. The reason why the E_{ii} value shifts is that the photo-excited electron and hole pair forms an exciton even at the room temperature, in which the attractive Coulomb interaction between the electron and hole (the exciton binding energy E_{bd}) or the repulsive Coulomb interaction between the photo-excited electrons and valence electrons (the self energy, Σ) are screened partially by the dielectric constants of the nanotube itself and the surrounding materials [8–12].

We have developed a computer program for calculating the exciton energies of a SWNT using the extended tight binding (ETB) method in which the ETB parameter set and the Coulomb interaction are evaluated by the wavefunction obtained by a first principles calculation [11, 13]. In the ETB exciton calculation, the Bethe–Salpeter equation is solved by diagonalizing a matrix in which the diagonal terms correspond to the pseudo-particle energy as a sum of the single particle energy E_{sp} and Σ, and the off-diagonal terms correspond to the mixing term with different k states by the Coulomb interaction so as to minimize the exciton energy [11]. Since $\Sigma > E_{bd} > 0$, the exciton energy $E_{ex} = E_{sp} + \Sigma - E_{bd}$ is slightly larger than E_{sp} in the all cases. Thus when the dielectric constant for the surrounding materials is large, E_{ex} decreases since the net Coulomb

interaction, $\Sigma - E_{\rm bd} > 0$, decreases. It is opposite to the situation of the conventional exciton energies in which the exciton energy increases with increasing dielectric constant.

Recent experimental results show many exciton spectra such as two-photon absorption spectra which give the excited exciton states [14, 15] and the energy differences between the bright and dark exciton states by the PL measurement under a magnetic field [16, 17]. Thus a direct comparison with many exciton energies are now available and this is important for checking the reliability of the exciton calculation and for understanding the physics of the environmental effect. In this paper, we calculated both the dark and bright exciton states or the exciton excited states to compare with experimental results.

In Section 2, we briefly explain the calculational method. In Section 3, we compare the calculated results for many kinds of exciton states with experimental results. In Section 4, a summary is given.

2 Method The exciton calculation program for a SWNT [11, 12] which consists of single-particle energy calculation by the ETB calculation [18], the Coulomb interaction calculation with use of the so-called Ohno's potential [8, 9], and the Bethe–Salpeter equation in which the Bloch states with wavevector k are mixed with one another so that we thus obtain the exciton energy and the spatially localized exciton wavefunction. As for the dielectric response of the π electron, we consider the polarization function $\Pi(q)$ within the random phase approximation [8, 9], while the dielectric response of the σ electrons and the surrounding materials is expressed by a single of dielectric constant κ. Dynamical screening of π electrons which is independent of the environmental effect, is thus considered in $\Pi(q)$ in which we can calculate E_{ii} values not only for semiconducting SWNTs but also for metallic SWNTs. However, we did not consider the elastic or inelastic scattering events of electrons for considering dielectric response, which may give upper limit of the response time. By adjusting the κ value to the experimental E_{ii} value of a given (n, m) SWNT including its environment, we can reproduce the experimental E_{ii} values for the SWNT. The experimental E_{ii} values, $E_{\rm exp}$ are observed from the Raman excitation profile for a given RBM spectra by changing $E_{\rm L}$ [4, 19–21]. We can thus assign each (n, m) value from the $(2n + m) =$ constant family pattern and from the different RBM frequencies for a given $(2n + m)$ family.

From the optimized κ values for many (n, m) SWNTs and for several environmental materials studied by the experiments, we here discuss the diameter dependent κ values which are useful for calculating the E_{ii} value for general surrounding materials. If we specify a range of E_{ii} energies, the SWNT diameter d_t, or one kind of surrounding material, we can get a better fitting function of κ, which will be reported in Ref. [21].

3 Calculated results Here we show calculated results for the exciton states of: (i) the bright exciton Kataura plot; (ii) the excited exciton states; and (iii) the difference between dark and bright exciton states. These exciton states are compared respectively, with: (i) resonance Raman spectroscopy; (ii) two-photon absorption spectroscopy [14, 15]; and (iii) single nanotube PL spectroscopy under a magnetic field [16, 17].

3.1 Bright exciton Kataura plot The bright exciton state is the spin-singlet, A_{1u} exciton state in which the k states near the K point and the $-k$ states near the K' point in the two dimensional (2D) Brillouin zone (BZ) of graphene are mixed anti-symmetrically with each other [22]. This mixing occurs via the inter-valley Coulomb interaction between the K point and the K' point states whose values are in the order of meV. Thus, as far as we discuss E_{ii} energies for RRS, the small inter-valley interaction can affect only the symmetry of the wavefunction, but not the value of E_{ii} itself very much. Since the ground states, the Hamiltonian, and the A_{1u} exciton state are, respectively, even, odd, and odd functions under the C_2 rotation for the axis perpendicular to the nanotube axis which exchanges A and B carbon atoms in the unit cell of graphene with each other, the dipole transition matrix elements become non-zero. On the other hand, the A_{1g} exciton state, in which the k states and the $-k$ states in the 2D BZ are mixed symmetrically with each other, becomes a dark exciton state.

In Fig. 1(a), we show the E_{ii} as a function of the SWNT diameter d_t as the bright exciton Kataura plot in which the dielectric constant κ is taken as a function of d_t as

$$\kappa = C \times \left(\frac{p}{d_t}\right)^{1.7} \tag{1}$$

where p denotes an integer and $p = 1$, 2, 3, 4, and 5 correspond to E_{11}^S, E_{22}^S, E_{11}^M, E_{33}^S, and E_{44}^S, respectively [3]. The p/d_t ratio represents the distance of the k point from the K point in the 2D BZ of graphene [23, 24], so that we can compare the κ values with different d_t and different E_{ii} in the same plot. In fact, the Coulomb interaction is known as a function of the distance of k from the K point in the 2D BZ [25, 26]. The formula in Eq. (1) is obtained by fitting the optimized κ values for each (n, m) SWNT to reproduce the experimental E_{ii} by Raman excitation profiles for several different conditions such as an as-grown sample of water-assisted (super-growth) chemical vapor deposition (CVD) SWNTs [19] and a HiPCO sample with sodium-dodecyl-sulfate (SDS) surfactants [4, 27]. as shown in Fig. 1(b). In Fig. 1(b), we plot the optimized κ values so as to reproduce the experimental E_{ii} values of the semiconducting SWNTs in a log–log plot of κ as a function of p/d_t. Here, each symbol denotes E_{11}^S (circle), E_{22}^S (cross), E_{33}^S (triangle), and E_{44}^S (square), respectively. Since the optimized κ values for E_{33}^S and E_{44}^S are smaller than those for E_{11}^S, E_{22}^S, we use two fitting functions (dashed lines) in which the constants C in Eq. (1) are 0.75 and 0.5 for E_{11}^S and E_{22}^S and for E_{33}^S and E_{44}^S, respectively. When we use the fitting function for κ, we get an accuracy of the energy difference between the experimental $E_{ii}^{\rm exp}$ and the calculated

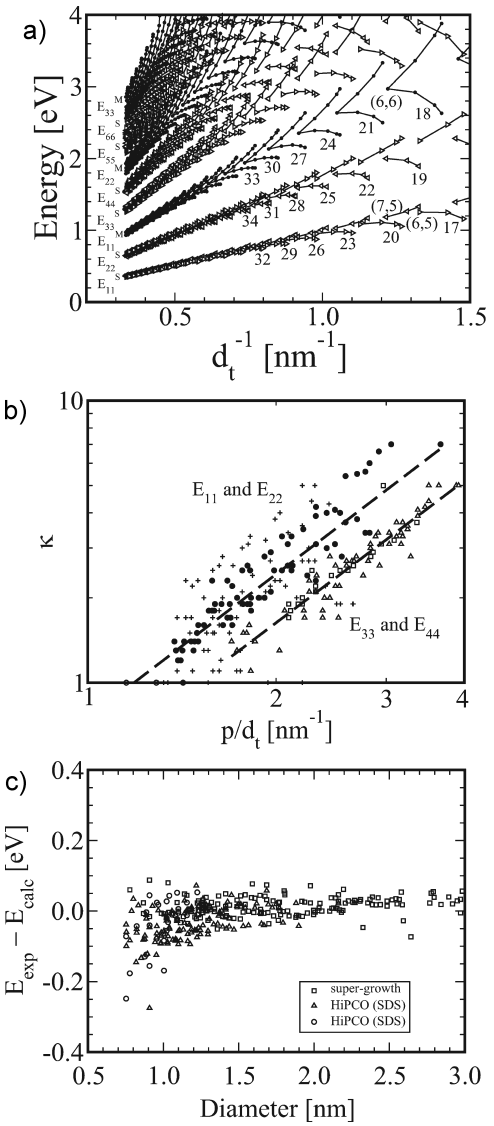

Figure 1 (a) Bright exciton Kataura plot, in which the numbers denote $2n + m$ family numbers for (n, m) SWNTs. (b) The optimized κ values which reproduce the experimental E_{ii} as a function of p/d_t, where p denotes an integer and $p = 1$, 2, 4, and 5 correspond to E_{11}^S (circles), E_{22}^S (crosses), E_{33}^S (triangles), and E_{44}^S (squares), respectively. The dashed lines are fitting functions shown in Eq. (1). (c) The energy difference between the experimental E_{ii} and the calculated E_{ii} using the fitting function of κ. Symbols denote as-grown samples of water-assisted (super-growth) CVD SWNTs (squares [19]) and SDS-wrapped HiPCO SWNTs (triangles [4] and circles [27]).

E_{ii}^{cal} values, $E_{ii}^{exp} - E_{ii}^{cal}$ which falls within ± 100 meV for a wide d_t range ($0.5 < d_t < 3.0$ nm) and for a wide energy range ($0.5 < E_{ii} < 3$ eV), as shown in Fig. 1(c), which is a sufficiently good fit for considering many SWNTs with different surfactants. It should be mentioned that $E_{ii}^{exp} - E_{ii}^{cal}$ is large for small d_t. For small d_t SWNTs, we should consider the effect that the effective mass of the electron and hole shows a large chiral angle dependence [25], which gives a chiral angle dependence for the E_{ii} values, which is the origin of the large observed deviation. However, in the present paper, we did not consider the chiral angle dependence for simplicity. In fact, the effect of the effective mass for different environmental materials does not give a consistent picture which improves the numerical accuracy in any case, which should be a future problem.

In Fig. 1(c), we consider two kinds of surfactants, such as an as-grown sample of water-assisted (super-growth) CVD SWNTs (squares, [19]) and SDS wrapped HiPCO SWNTs (triangles [4] and circles [27]). If we specify one of these samples, we can have other C values for the specified samples, which give better results [21]. Here, we focus on our proposal that a general formula of a diameter dependent κ value is useful for describing unknown surfactant materials.

The reason why we get a smaller C value for E_{33}^S and E_{44}^S than for E_{11}^S and E_{22}^S is that the exciton binding energy is larger for E_{33}^S and E_{44}^S and that the exciton size is smaller at the same time in real space. Thus the E_{33}^S and E_{44}^S excitons feel the dielectric constant of the surfactant less than those for E_{11}^S and E_{22}^S. This is why the effective value of κ is smaller. The κ value may consist of the dielectric constant of a SWNT κ_{tube} and that of the surrounding materials κ_{env} [6]. In a previous paper, we showed that κ is expressed by

$$\frac{1}{\kappa} = \frac{C_1}{\kappa_{tube}} + \frac{C_2}{\kappa_{env}}, \tag{2}$$

in which C_1 and C_2 are diameter-dependent coefficients, respectively [6]. Except for isolated SWNTs, we generally expect $\kappa_{env} > \kappa_{tube}$. For a large d_t, the contribution of κ_{env} becomes small, which is one reason why the κ value decreases with increasing d_t. A power of $(p/d_t)^{1.7}$ which is obtained in the process of the fitting procedure is close to 2, which we discussed in a previous paper [6]. The deviation from the value 2 might come from the fact that the exciton size itself increases with increasing diameter, and thus the d_t^{-2} dependence is slightly relaxed. This is consistent with the scaling properties of the exciton [22]. It will be a future problem to obtain this factor by considering some analytic expression for the electric field produced by an exciton.

3.2 2g exciton states Maultzsch et al. [14] and Dukovic et al. [15] have measured the two-photon absorption, in which the two-photon excitation to the 2g exciton states A_{2g} brings the subsequent relaxation to the bright exciton states A_{1u} and PL emission from the A_{1u} states. Even though the A_{2g} states are optical forbidden states for a one-photon process, we can determine the position of A_{2g} by the two-photon measurement by changing the laser excitation energy E_L.

In Fig. 2(a), we plot the calculated E_{11}^{1u} (circles) and E_{11}^{2g} (crosses) as a function of d_t, in which we use the constant value of $\kappa = 2.7$ by fitting the experimental values. Since we consider only E_{11} and only for a small diameter region from 0.6 to 1.2 nm, a constant value of κ is sufficient to reproduce the experimental results. When we plot the energy difference of $E_{11}^{2g} - E_{11}^{1u}$ (see Fig. 2(b)), the deviation from the experimental results only show chiral angle dependence that we did not consider in this paper. The integers in Fig. 2(a) are

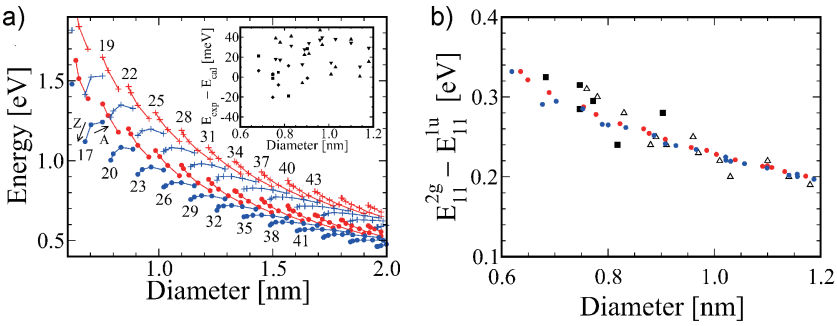

Figure 2 (online color at: www.pss-b.com) (a) E_{11}^{1u} (circles) and E_{11}^{2g} (crosses) are plotted as a function of d_t. The numbers denote $(2n+m)$ family numbers. The κ value fitted to the experimental data is 2.7. Red and blue symbols denote, respectively, type I and II semiconducting SWNTs. The inset to Fig. 2(a) shows the energy difference of $E_{ii}^{exp} - E_{ii}^{cal}$ for E_{11}^{1u} (diamonds and up triangles, respectively, for the experimental data by Maultzsch et al. [14] and Dukovic et al. [15]) and E_{11}^{2g} (squares and down triangles). (b) The calculated $E_{11}^{2g} - E_{11}^{1u}$ (circles) as a function of d_t. Squares and up triangles are the experimental results by Maultzsch et al. [14] and Dukovic et al. [15].

$(2n+m)$ family numbers for (n,m) SWNTs. The same $(2n+m)$ family number corresponds to SWNTs with a similar d_t to one another, and thus the change within the same family shows a chirality dependence of the exciton energy, which we call a family pattern. Depending on the value of $\mathrm{mod}(2n+m,3) = 1$ or 2, type I and II semiconductor SWNTs are classified, in which we show red and blue symbols, respectively. Within a family, A and Z denote the chiral angle close to armchair or zigzag SWNTs, respectively.

The inset of Fig. 2(a) shows the energy difference of $E_{ii}^{exp} - E_{ii}^{cal}$ for E_{11}^{1u} (diamonds and up triangles, respectively, for the experimental data by Maultzsch et al. [14] and Dukovic et al. [15]) and E_{11}^{2g} (squares and down triangles). All the data for $E_{ii}^{exp} - E_{ii}^{cal}$ are within ± 50 meV for a constant κ, not only for the bright exciton states but also for the excited exciton states. Since the diameter range for the experimental data is relatively small and since the data is only for E_{11}^{S} values, a fitted κ $(= 2.7)$ value to the experimental data is sufficient for reproducing the experimental data.

Since the family pattern for E_{11}^{1u} and E_{11}^{2g} are similar to each other, thus the difference of $E_{11}^{2g} - E_{11}^{1u}$ shows only a diameter dependence, as shown by the red or blue circles in Fig. 2(b) for type I and II SWNTs, respectively. In Fig. 2(b), we compare the calculated results with the experimental results for $E_{11}^{2g} - E_{11}^{1u}$ by Maultzsch et al. (squares) [14] and Dukovic et al. (triangles) [15]. We can show that the difference is sufficiently small (± 30 meV) for all diameters. Although the calculated results for $E_{11}^{2g} - E_{11}^{1u}$ do not show any chiral angle dependence, the experimental results show some fluctuations of their values which can not be explained by the chirality dependence of the exciton states. We think that these fluctuations may come from the local environmental effect of the sample, since the sample is not composed of isolated SWNTs and the local environment is fluctuating on a scale greater than the wavelength of the light. In fact, the sample is treated by SDS in D_2O [14] or by aqueous poly(maleic acid/octyl vinyl ether) [15]. It should be interesting in the future to carry out two-photon measurements and to plot $E_{11}^{2g} - E_{11}^{1u}$ for more SWNTs.

3.3 The difference between dark and bright exciton states When the magnetic field is applied parallel to the nanotube axis, the cutting lines in the 2D Brillouin zone are shifted in the direction perpendicular to the cutting lines [1, 28] and thus the time-reversal symmetry between k and $-k$ is broken. In this case, the dark exciton states start to be optically allowed [29, 30], even for a small magnetic field, such as 5T [16, 17].

In Fig. 3(a), we plot the energy difference between the dark and bright exciton states $\Delta_{bd} = E_{11}^{1u} - E_{11}^{1g}$ for E_{11}^{S} as a function of d_t. In this calculation we simply adopted a constant $\kappa = 2.22$ for simplicity, since we focus our calculation on the smaller diameter region and lower energy range. In fact, the sample consists of bundles [16] which we fitted to $\kappa = 2.22$ for E_{22}^{S} [11] or isolated SWNTs [17] in which the κ should be smaller than 2.22. Red and blue symbols denote $\mathrm{mod}(2n+m,3) = 1$ and 2 (type I and II) SWNT families, respectively. The green symbols with error bars are the experimental results which are observed for isolated, suspended SWNT PL spectroscopy under the magnetic field by Matsunaga et al. [17]. The experimental energies are smaller for all cases than the calculated results. Since Δ_{bd} is closely related to the relative strength of the inter-valley and intra-valley Coulomb interaction, the present results may show that the intervalley Coulomb interaction is underestimated in the present calculation.

In Fig. 3(b), we show the energy difference between the dark and bright exciton energies Δ_{bd} as a function of κ for a (9,7) SWNT. The Δ_{bd} does not depend much on κ and thus we could not find a reasonable κ value which reproduces the experimental results, since κ works equally for the intra-valley and inter-valley Coulomb interactions. Thus within our treatment of the calculation, it seems to be difficult for us to fit Δ_{bd} merely by changing the κ value.

Ando [29] showed in the effective mass approximation calculation that Δ_{bd} depends on the ratio of the short-range (intra-valley) Coulomb w_1 and the long-range (inter-valley) Coulomb interaction w_2, that is w_1/w_2, in q space, in which the bright exciton energy increases with increasing w_1/w_2, while the dark exciton energy slightly decreases with increasing w_1/w_2. Thus, in order to obtain a smaller Δ_{bd}, a relatively smaller w_1/w_2 is needed. In future works, we should consider a Coulomb interaction which reproduces not only the bright exciton states, but also the dark exciton states.

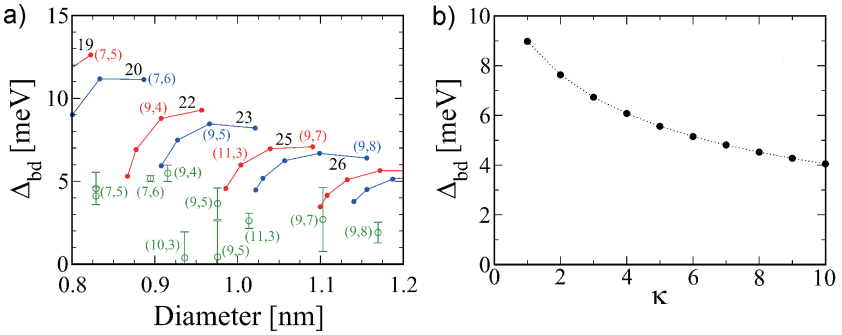

Figure 3 (online color at: www.pss-b.com) (a) The energy difference between the bright and dark exciton states $\Delta_{bd} = E_{11}^{1u} - E_{11}^{1g}$ for E_{11}^{S} states. Red and blue symbols denote the calculated results for type I and II semiconducting SWNTs. The green symbols with error bars are the experimental results observed by Matsunaga et al. [17]. (b) The calculated energy difference between the bright and dark exciton states as a function of the dielectric constant for a (9, 7) SWNT.

We can see the family pattern for type I and II SWNTs in Fig. 3(a) which implies a chirality dependence of Δ_{bd}. However, compared with the cases of E_{11}^{1u} for which the family pattern of E_{11}^{1u} from armchair to zigzag chiral angle appear in the opposite direction to each other for type I and II SWNTs, the family pattern of Δ_{bd} appears in the same direction for type I and II SWNTs. The Δ_{bd} close to the armchair chiral angle has a maximum value within a family. The reason for this effect is not clear at the present stage.

4 Summary In summary, the diameter dependent κ values reproduce the bright exciton and the excited exciton energies within reasonable accuracy for a wide range of diameters and energies. However, the energy difference between bright and dark exciton states does not reproduce the experiment well, for the same κ value. However, the chirality dependent Δ_{bd} reproduces the experimental data. Thus, we think that we should consider an evaluation of the Coulomb interaction as a function of the q vector in the near future.

Acknowledgements P.T.A. and A.J. acknowledge financial support by FAPEMIG and CNPq. M.S.D. acknowledges support from NSF grants (no. DMR07-01497). R.S. thanks Prof. J.-L. Sauvajol, Prof. J. Kono, and Prof. K. Matsuda for providing the experimental exciton energy data. R.S. acknowledges support from NEXT grants (no. 20241023). K.S. is supported by JSPS Research Fellowships for Young Scientists (no. 20-4594).

References

[1] R. Saito, G. Dresselhaus, and M. S. Dresselhaus, Physical Properties of Carbon Nanotubes (Imperial College Press, London, 1998).
[2] H. Kataura, Y. Kumazawa, Y. Maniwa, I. Umezu, S. Suzuki, Y. Ohtsuka, and Y. Achiba, Synth. Met. **103**, 2555 (1999).
[3] R. Saito, G. Dresselhaus, and M. S. Dresselhaus, Phys. Rev. B **61**, 2981 (2000).
[4] C. Fantini, A. Jorio, M. Souza, M. S. Strano, M. S. Dresselhaus, and M. A. Pimenta, Phys. Rev. Lett. **93**, 147406 (2004).
[5] Y. Ohno, S. Iwasaki, Y. Murakami, S. Kishimoto, S. Maruyama, and T. Mizutani, Phys. Rev. B **73**, 235427 (2006).
[6] Y. Miyauchi, R. Saito, K. Sato, Y. Ohno, S. Iwasaki, T. Mizutani, J. Jiang, and S. Maruyama, Chem. Phys. Lett. **442**, 394 (2007).
[7] P. T. Araujo and A. Jorio, Phys. Status Solidi B **245**, 2201 (2008).
[8] T. Ando, J. Phys. Soc. Jpn. **66**, 1066 (1997).
[9] T. Ando, J. Phys. Soc. Jpn. **73**, 3351 (2004).
[10] C. D. Spataru, S. Ismail-Beigi, L. X. Benedict, and S. G. Louie, Phys. Rev. Lett. **92**, 077402 (2004).
[11] J. Jiang, R. Saito, G. G. Samsonidze, A. Jorio, S. G. Chou, G. Dresselhaus, and M. S. Dresselhaus, Phys. Rev. B **75**, 0354073 (2007).
[12] M. S. Dresselhaus, G. Dresselhaus, R. Saito, and A. Jorio, Annu. Rev. Phys. Chem. **58**, 719–747 (2007).
[13] J. Jiang, R. Saito, K. Sato, J. S. Park, G. G. Samsonidze, A. Jorio, G. Dresselhaus, and M. S. Dresselhaus, Phys. Rev. B **75**, 035405 (2007).
[14] J. Maultzsch, R. Pomraenke, S. Reich, E. Chang, D. Prezzi, A. Ruini, E. Molinari, M. S. Strano, C. Thomsen, and C. Lienau, Phys. Rev. B **72**, 241402 (2005).
[15] G. Dukovic, F. Wang, D. Song, M. Y. Sfeir, T. F. Heinz, and L. E. Brus, Nano Lett. **5**, 2314 (2005).
[16] A. Srivastaba, H. Htoon, V. I. Klimov, and J. Kono, Phys. Rev. Lett. **101**, 087402 (2008).
[17] R. Matsunaga, K. Matsuda, and Y. Kanemitsu, Phys. Rev. Lett. **101**, 147404 (2008).
[18] G. G. Samsonidze, R. Saito, N. Kobayashi, A. Grüneis, J. Jiang, A. Jorio, S. G. Chou, G. Dresselhaus, and M. S. Dresselhaus, Appl. Phys. Lett. **85**, 5703 (2004).
[19] P. T. Araujo, S. K. Doorn, S. Kilina, S. Tretiak, E. Einarsson, S. Maruyama, H. C. M. A. Pimenta, and A. Jorio, Phys. Rev. Lett. **98**, 067401 (2007).
[20] T. Michel, M. Paillet, J. C. Meyer, V. N. Popov, L. Henrard, and J. L. Sauvajol, Phys. Rev. B **75**, 1554325 (2007).
[21] P. Araujo, A. Jorio, M. S. Dresselhaus, K. Sato, and R. Saito, Phys. Rev. Lett., in press.
[22] V. Perebeinos, J. Tersoff, and P. Avouris, Phys. Rev. Lett. **92**, 257402 (2004).
[23] R. Saito, K. Sato, Y. Oyama, J. Jiang, G. G. Samsonidze, G. Dresselhaus, and M. S. Dresselhaus, Phys. Rev. B **71**, 153413 (2005).
[24] G. G. Samsonidze, R. Saito, A. Jorio, M. A. Pimenta, A. G. Souza Filho, A. Grüneis, G. Dresselhaus, and M. S. Dresselhaus, J. Nanosci. Nanotechnol. **3**, 431 (2003).
[25] K. Sato, R. Saito, J. Jiang, G. Dresselhaus, and M. S. Dresselhaus, Phys. Rev. B **76**, 195446 (2007).
[26] K. Sato, R. Saito, J. Jiang, G. Dresselhaus, and M. S. Dresselhaus, Vib. Spectrosc. **45**, 89 (2007).
[27] E. H. Haroz, S. M. Bachilo, R. B. Weisman, and S. K. Doorn, Phys. Rev. B **77**, 125405 (2008).
[28] R. Saito, G. Dresselhaus, and M. S. Dresselhaus, Phys. Rev. B **50**, 14698 (1994); Phys. Rev. B **53**, 10408 (1996).
[29] T. Ando, J. Phys. Soc. Jpn. **75**, 024707 (2006).
[30] J. Shaver, J. Kono, O. Portugall, V. Krstic, G. L. J. A. Rikken, Y. Miyauchi, S. Maruyama, and V. Perebeinos, Nano Lett. **7**, 1851 (2007).